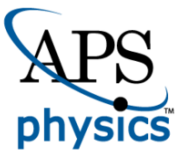

Interaction-Driven Shift and Distortion of a Flat Band in an Optical Lieb Lattice

Hideki Ozawa, Shintaro Taie, Tomohiro Ichinose, and Yoshiro Takahashi

Phys. Rev. Lett. **118**, 175301 — Published 25 April 2017

DOI: 10.1103/PhysRevLett.118.175301

Interaction-Driven Shift and Distortion of a Flat Band in an Optical Lieb Lattice

Hideki Ozawa,[1,*] Shintaro Taie,[1] Tomohiro Ichinose,[1] and Yoshiro Takahashi[1]

[1] *Department of Physics, Graduate School of Science, Kyoto University, Japan 606-8502*

(Dated: April 6, 2017)

We report the momentum-resolved measurement of Bloch bands in an optical Lieb lattice for a Bose-Einstein condensate (BEC). A BEC in the lattice is transported to a desired quasimomentum by applying a constant force. The energy dispersion of the lowest band is obtained by integrating measured group velocities. We also measure the gap from the lowest band to the higher bands with the same quasimomentum, which can be extracted from the oscillation of the sublattice populations after preparing a superposition of the band eigenstates. We show that the experimental results agree with a band calculation based on the Bogoliubov approximation. It is revealed that the second band, which should be flat in a single-particle description, is shifted and, in particular, distorted around the Brillouin zone (BZ) edge as the interaction strength increases.

PACS numbers: 67.85.-d, 03.75.Kk

Flat bands possess macroscopic level degeneracy because of their dispersionless band. Flat bands appear in various contexts of condensed-matter physics, ranging from the Landau levels of two-dimensional electrons [1], edge states of graphene [2] to unconventional superconductors [3]. Intriguingly, such flatten band structure shows wide range of many-body phenomena from supersolidity [4] to flat-band ferromagnetism [5–7]. In addition, flat bands with nontrivial topological properties have attracted much attention for their application in realizing a fractional quantum Hall state without Landau levels [8–10].

In a special lattice structure such as kagome, sawtooth and Lieb lattices, the destructive interference of the tunneling induces frustration of kinetic energy and results in a bulk flat band. For bosonic systems, a fascinating question has been considered whether condensation is stable in a flat band. In a kagome lattice, it is theoretically investigated that an interaction makes the energy at the K-point which corresponds to the corner of the hexagonal first BZ lowest in a flat band [11]. Recently, several lattice structures with a flat band have been realized in optical lattices [12, 13], photonic lattices [14–16] and a polaritonic system [17]. Above all, ultracold atoms in optical lattices have great advantages in terms of their simplicity and dynamical controllability of system parameters such as tunneling amplitude and on-site interaction in the Hubbard regime [18]. In ultracold atom experiments, a band structure of an optical lattice can be measured in momentum-resolved manner by Bragg spectroscopy [19] and a combination of Bloch oscillation and Stückelberg interferometry [20]. The former method requires a continuous change of the angle between the driving laser beams. In the latter method, only the gap between the 1st band and 2nd band can be measured.

In this paper, we report the momentum-resolved measurement of the lowest three Bloch bands for an interacting array of BEC trapped in an optical Lieb lattice (Fig. 1(a)). Three-sublattice structure (A, B, and C) of the Lieb lattice gives rise to three s-orbitals described as

$$\begin{aligned} |\boldsymbol{q}, 1\mathrm{st}\rangle &= \frac{1}{\sqrt{2}}\left(|\boldsymbol{q}, A\rangle + \sin\theta_q\,|\boldsymbol{q}, B\rangle + \cos\theta_q\,|\boldsymbol{q}, C\rangle\right) \\ |\boldsymbol{q}, 2\mathrm{nd}\rangle &= \cos\theta_q\,|\boldsymbol{q}, B\rangle - \sin\theta_q\,|\boldsymbol{q}, C\rangle \\ |\boldsymbol{q}, 3\mathrm{rd}\rangle &= \frac{1}{\sqrt{2}}\left(|\boldsymbol{q}, A\rangle - \sin\theta_q\,|\boldsymbol{q}, B\rangle - \cos\theta_q\,|\boldsymbol{q}, C\rangle\right) \end{aligned} \quad (1)$$

where $|\boldsymbol{q}, S\rangle$ ($S = A, B, C$) is a plane wave on a sublattice S with quasimomentum $\boldsymbol{q}$, and θ_q satisfies $\tan\theta_q = \cos(q_x d/2)/\cos(q_z d/2)$. The resulting single-particle energy spectrum has a flat band as the second band and a Dirac cone at the corner of the Brillouin zone (Fig. 1 (b)). To investigate the dispersion relation, a BEC in the lattice is transported to various quasimomenta by applying a constant force [21]. The dispersion of the lowest band is acquired by integrating group velocity measured from matter-wave interference patterns (Fig. 1 (c)). For the higher bands, we measure the gap from the lowest band (Fig. 1 (d)). High controllability of the optical lattice enables us to prepare the precise superposition of band eigenstates [13]. Once such a state is introduced into the Lieb lattice, the sublattice population starts oscillation whose frequency corresponds to the band gap. This work sheds light on the important role of the interaction in significantly modifying the Bloch band including a flat band in the Lieb lattice.

We begin with describing our experimental setup. A nearly pure condensate of ytterbium (^{174}Yb) is optically trapped using far-off-resonant trap (FORT) laser beams. An optical Lieb lattice is then adiabatically ramped up and the BEC is located at quasimomentum $\boldsymbol{q} = \boldsymbol{0}$ (Γ point) of the lowest band. Our optical Lieb lattice potential is given by

$$\begin{aligned} V(x,z) = &-V_{\mathrm{long}}^{(x)}\cos^2(k_{\mathrm{L}}x) - V_{\mathrm{long}}^{(z)}\cos^2(k_{\mathrm{L}}z) \\ &- V_{\mathrm{short}}^{(x)}\cos^2(2k_{\mathrm{L}}x) - V_{\mathrm{short}}^{(z)}\cos^2(2k_{\mathrm{L}}z) \\ &- V_{\mathrm{diag}}\cos^2(k_{\mathrm{L}}(x-z)+\pi/2) \end{aligned} \quad (2)$$

where z indicates the direction of gravity. $k_{\mathrm{L}} = 2\pi/\lambda$ is a wavenumber of a long lattice for which we choose

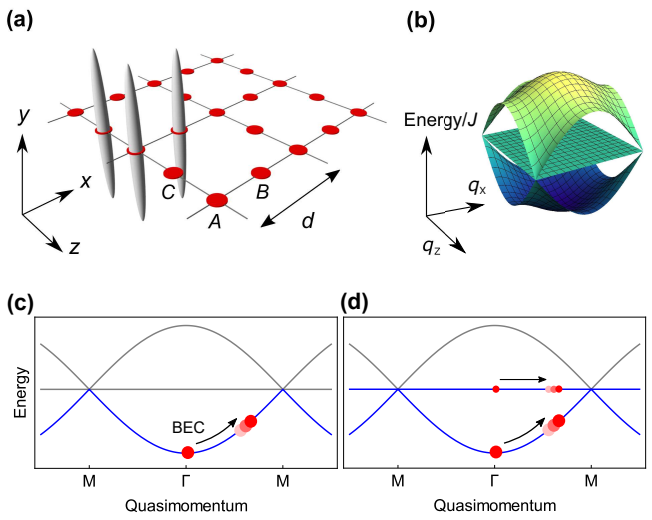

FIG. 1. (Color online) (a) Schematic of Lieb lattice. In our system, the atoms are weakly trapped along the y direction, and distribute like tubes as described in gray in the figure. (b) Band structure of Lieb lattice in single-particle description. (c) Method for measuring dispersion of the lowest band. Red circles indicate atomic cloud. After transporting a BEC to a desired quasimomentum, we measure the group velocity and integrate the results. (d) Method for measuring a band gap in momentum-resolved manner. We prepare the superposition of band eigenstates, transport the atoms to a desired quasimomentum, and measure an oscillation frequency of the sublattice population.

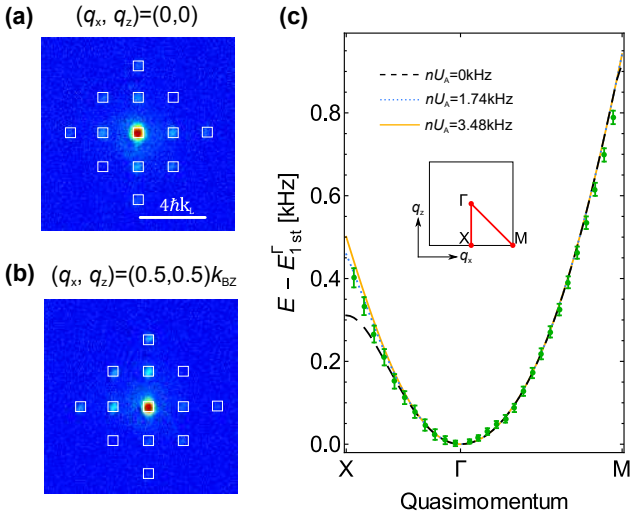

FIG. 2. (Color online) (a), (b) Absorption images at quasimomentum $(q_x, q_z) = (0, 0)$ and $(0.5, 0.5)k_{\mathrm{BZ}}$ respectively, where k_{BZ} corresponds to the quasimomentum at the BZ edge. The images are taken after a TOF of 14ms. We restrict the integration region within the white squares in which the atoms are mostly detected. (c) Dispersion of the 1st band of optical Lieb lattice $(s_{\mathrm{long}}, s_{\mathrm{short}}, s_{\mathrm{diag}}) = (13, 13, 15.5)$. The experimental data are denoted as green circles. The inset shows the first BZ. Dashed black line is single-particle theory. Dotted blue line is the calculation for half of the maximum number density. Solid yellow line is for the maximum number density. The vertical axis shows the energy difference from the 1st band energy at Γ for each interaction strength. Error bar means the standard deviation of three independent scans.

$\lambda = 1064$ nm. In the following, we specify each lattice depth as $(s_{\mathrm{long}}, s_{\mathrm{short}}, s_{\mathrm{diag}}) = (V_{\mathrm{long}}, V_{\mathrm{short}}, V_{\mathrm{diag}})/E_{\mathrm{R}}$, where $E_{\mathrm{R}} = \hbar^2 {k_{\mathrm{L}}}^2/(2m)$ is the recoil energy and m is the atomic mass of ^{174}Yb. In the y direction which is perpendicular to the Lieb lattice plane, the atoms are weakly confined in a harmonic trap, resulting in 2D array of 1D tubes as illustrated in Fig. 1 (a). To move the atoms in the reciprocal space, we utilize two kinds of external forces. One is a gravitational force acting in $\Gamma(q_x = 0, q_z = 0)$ to $\mathrm{X}(q_x = k_{\mathrm{BZ}}, q_z = 0)$ direction, which can be applied by turning off the FORT potential, where $k_{\mathrm{BZ}} = \pi/d = k_{\mathrm{L}}$. The other is a dipole force due to the potential gradient of a Gaussian beam with the beam waist of about 50 μm and about 1 GHz red detuning from the resonance of the $^1S_0$ - $^3P_1$ transition ($\lambda = 556$ nm) acting in Γ to $\mathrm{M}(q_x = k_{\mathrm{BZ}}, q_z = k_{\mathrm{BZ}})$ direction.

In the presence of a constant external force $\boldsymbol{F}$, which is weak enough not to induce interband transitions, a given band eigenstate $|\boldsymbol{q}(0), n\rangle$ evolves to $|\boldsymbol{q}(t), n\rangle$ according to $\boldsymbol{q}(t) = \boldsymbol{q}(0) + \boldsymbol{F}t/\hbar$ after a time t [21]. The group velocity in $|\boldsymbol{q}(t), n\rangle$ is related to the band eigenenergy $E_n(\boldsymbol{q}(t))$ as [22]

$$\langle \boldsymbol{v} \rangle_n (\boldsymbol{q}(t)) = \frac{1}{\hbar} \frac{\mathrm{d}E_n(\boldsymbol{q}(t))}{\mathrm{d}\boldsymbol{q}}. \tag{3}$$

In the following, we reconstruct the dispersion of the lowest band by integrating the group velocities detected via time-of-filight (TOF) measurements [23, 24]. From a TOF image, we can observe the velocity distribution of atomic cloud $n(v_x, v_z)$, which is once integrated in the direction perpendicular to the Lieb lattice plane. Using the velocity distribution, the group velocity is given as $\langle \boldsymbol{v} \rangle = \int \mathrm{d}v_x \mathrm{d}v_z \, \boldsymbol{v} n(v_x, v_z)$. When extracting the group velocity from TOF images, we reduce the influence of the background noise in the region where the atoms are not populated by restricting the region of integration into the squares as in Fig. 2 (a), (b), whose centers correspond to $\hbar(q_x(t), q_z(t)), \hbar(q_x(t) \pm 2k_{\mathrm{L}}, q_z(t) \pm 2k_{\mathrm{L}}), \hbar(q_x(t), q_z(t) \pm 4k_{\mathrm{L}}), \hbar(q_x(t) \pm 4k_{\mathrm{L}}, q_z(t))$ and the width is $\simeq \hbar k_{\mathrm{L}}/3$. Measured group velocity at each quasimomentum is integrated in a trapezoidal approximation: $E(\boldsymbol{q})/\hbar = \int_{\boldsymbol{0}}^{\boldsymbol{q}} \mathrm{d}\boldsymbol{q}' \cdot \langle \boldsymbol{v} \rangle (\boldsymbol{q}') \sim \Sigma_{i=0}^{q'(i)=q} \mathrm{d}q' (\langle v \rangle (i+1) + \langle v \rangle (i))/2$.

When the BEC in the lowest band experiences a weak external force, the whole condensate occupies a single band at a single wavenumber. We compare the experimental data with Gross-Pitaevskii equation (GPE) in a tight-binding approximation (See S.1 in Supplementary Material [25]). Whereas the eigenstates given in Eq.(1) assume that tunneling occurs only between the nearest neighbors, there exists tunneling to the next nearest neighbors or in the diagonal direction in a shallow

optical lattice potential. We fit the tunneling parameters so that the resulting tight-binding model reproduces the band calculated by using optical lattice potentials. Wannier function is also determined by the optical lattice potential (See [13, 25]). We compare the experimental results with a band calculation with such realistic Hubbard parameters.

Figure 2 (c) shows the dispersion of the lowest band for the lattice depth of $(s_{\rm long}, s_{\rm short}, s_{\rm diag}) = (13, 13, 15.5)$. At this lattice depth, the atoms are in a superfluid state and not in a Mott-insulating state. In our system, an atom density has spatial dependence due to a weak harmonic confinement by laser beams. The trap frequencies of FORT and optical lattice are $(\omega_x, \omega_y, \omega_z)/2\pi = (129, 46.2, 151)$ Hz. Assuming a local density approximation, we can calculate the density distribution of atoms $n(\mu, r)$ in the optical lattice by determining chemical potential μ from the total atom number, which is $N = 2.1(1) \times 10^4$ (See S.3 in [25]). The Thomas-Fermi radii are $(r_x, r_y, r_z) = (3.07, 8.58, 2.62)$ μm. At the trap center, the mean-field interaction amounts to $nU_A/J = 8.06$, where U_A is the interaction strength on the A-sublattice. In Fig. 2 (c), band calculations for the maximum density and half of it are plotted in addition to a single-particle theory. Note that the 1st band energy at Γ ($E^{\Gamma}_{\rm 1st}$) of each interaction strength is subtracted to adjust the energy offset. The experimental data are in excellent agreement with the theoretical analysis. While the band dispersion along the Γ-M is robust against interaction, the band energy is slightly shifted up around the X point compared with the non-interacting case. This can be accounted by the concentration of the wave function on the A- and B-sites at this point.

Next, we describe the band gap measurement. Initially, a BEC is prepared as a superposition of eigenstates for the optical Lieb lattice of $(s_{\rm long}, s_{\rm short}, s_{\rm diag}) = (13, 13, 15.5)$. The overlap between the initial state and the eigenstates of higher bands is set to 10 %, which is small enough for the measured band gap not to depend on the higher band fraction (See S.4 in [25]). The initial lattice depths are $((s^x_{\rm long}, s^z_{\rm long}), s_{\rm short}, s_{\rm diag}) = ((12.31, 14.01), 6.84, 15.24)$ for the 1st-2nd band gap (E_{2-1}) measurement and $(s_{\rm long} = s^x_{\rm long} = s^z_{\rm long}, s_{\rm short}, s_{\rm diag}) = (12.49, 13.08, 17.82)$ for the 1st-3rd band gap (E_{3-1}) measurement. After changing the lattice configuration into the Lieb lattice suddenly, we move the BEC in the reciprocal space by applying a constant force. During the subsequent holding time, the relative phase between band eigenstates evolves at the frequency of the band gap, resulting in oscillations of the sublattice populations. To observe the real-space dynamics, we perform projection measurement of the occupation number in each sublattice, which we call sublattice mapping [13]. In this method, we change the lattice potential to $(s_{\rm long}, s_{\rm short}, s_{\rm diag}) = (8, 20, 0)$, where the lowest three bands consist of the A-, B-, and C-sublattice, respectively. This maps out sublattice occupations to band occupations, which can be measured by band mapping technique.

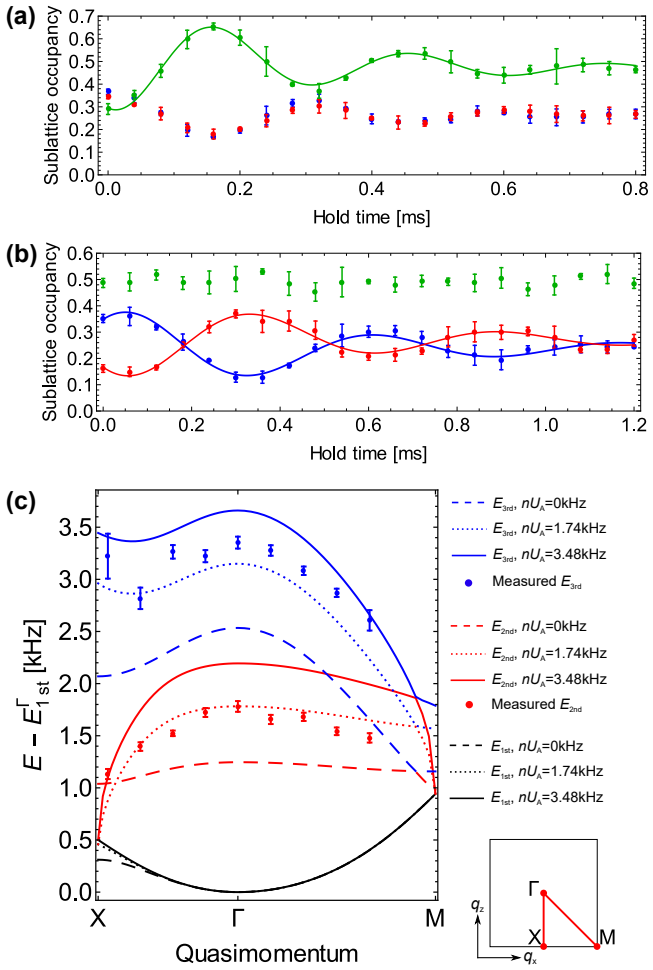

FIG. 3. (Color online) (a), (b) Oscillation of sublattice population at Γ point according to (a)E_{3-1} and (b) E_{2-1}, respectively. First, we load a BEC into an optical lattice the configuration of which is different from that of a Lieb lattice. In this way we create a superposition of (a) the 1st and 3rd or (b) the 1st and 2nd band eigenstates of the Lieb lattice. Next, we suddenly change the lattice configuration into the Lieb lattice, and take various hold time. We observe the temporal change of the sublattice populations obtained by the projection measurement described in the text. Each sublattice occupancy is normalized by the summation over all of the sublattice occupancy. Green, blue and red circles are A-, B-, and C-sublattice population, respectively. Error bar shows the standard deviation of three independent scans. Solid lines are fits to the data with damped sine functions(4). (c) The lowest three bands in the optical Lieb lattice of $(s_{\rm long}, s_{\rm short}, s_{\rm diag}) = (13, 13, 15.5)$. Red and blue circles are the reconstructed 2nd and 3rd band energies, respectively. Error bars mean the fitting errors. Dashed lines are the predictions based on a single-particle theory. Dotted and solid lines are the calculations including the interaction based on the BdGE with the half and maximum densities, respectively.

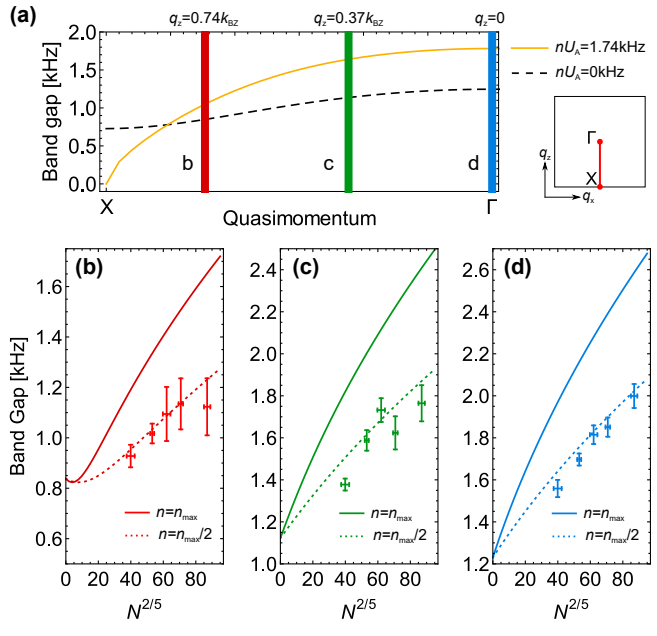

FIG. 4. (Color online) (a) Band gaps from the lowest band to the 2nd band. Dashed black line is the prediction on the single particle theory of the Lieb lattice potential $(s_{\rm long}, s_{\rm short}, s_{\rm diag}) = (13, 13, 15.5)$. Solid yellow line is the calculation including the interaction based on the BdGE. Thick red, green and blue lines respectively show the quasimomenta $q_z = 0.74k_{\rm BZ}, 0.37k_{\rm BZ}$, and 0 at which we have investigated the density dependence of the band gaps. (b), (c), (d) Band gap versus the atom number for $q_z = 0.74k_{\rm BZ}, 0.37k_{\rm BZ}, 0$, respectively. Solid and dotted lines show the calculations including the interaction based on the BdGE for the maximum and half densities, respectively. Error bars indicates the fitting errors.

When the superposition of the 1st and 3rd bands is prepared as an initial state, all of the sublattice population oscillate because the wave functions of 1st and 3rd bands spread over all the sublattices. On the other band, since the eigenstate of the 2nd band has no amplitude on A-sublattice, only B- and C-sublattice populations oscillate in the case of the superposition of the 1st and 2nd bands as an initial state. Therefore, we extract the band gap E_{3-1} from the frequency of A-sublattice oscillation (Fig. 3 (a)) and E_{2-1} from the mean of frequencies of B- and C-sublattice oscillations (Fig. 3 (b)). Note that the populations at B- and C-sublattices in Fig. 3 (a) evolve in the same way, because both of $|\Gamma, B\rangle$ and $|\Gamma, C\rangle$ always have the same coefficient in the superposed state. We fit the oscillation of sublattice population with our empirical model function

$$F(t) = a\, e^{-t/\tau} \sin(2\pi f t + b) + c \qquad (4)$$

where a, b, c, f, τ are fitting parameters.

In Fig. 3(c) we show the experimentally determined band energies (solid circles) in the optical Lieb lattice. The higher band energies are obtained from the combination of the energy gaps and the energy of the lowest band described above. The dashed lines are the results of the calculations based on a single particle theory. It is clear that the experimentally determined energies are significantly deviated, in particular, up-shifted and distorted, from the calculated bands, which should be ascribed as the interaction-driven effect. Note that a direct tunneling between B- and C-sublattices which exists in our Lieb lattice system distorts the flat band even in the single-particle limit. Theoretically, a Bloch state with a small fraction of higher bands is regarded as the state after the weak excitation from the lowest band. Therefore, we use the Bogoliubov-de Gennes equation (BdGE) to estimate the interaction effect on the energy gap (See S.2 in [25]). The dotted and solid curves show the results of the calculations with two different interaction strengths, respectively. Our calculation shows, in particular, that the band gaps or excitation energies around the center of BZ becomes larger as the interaction increases. On the contrary, the gap to the 2nd band becomes closed around the BZ edge of X point, as the interaction increases. We interpret this behavior as follows. At X point, $\cos(\theta_{\rm X}) = 0$ and $\sin(\theta_{\rm X}) = 1$, and thus the Bloch wave function of the 1st band has no spatial overlap with that of the 2nd band. Therefore, the excited atoms do not interact with the atoms in the lowest band, resulting in the smaller band gap as the interaction energy increases in the lowest band. On the other hand, because the 3rd band has large spatial overlap with the 1st band, the energy necessary to excite a particle to the 3rd band gets larger as the interaction increases. Note that along the Γ-M direction, $\cos(\theta_q) = \sin(\theta_q) = 1/\sqrt{2}$, and thus the 2nd band remains flat because the sublattice distribution does not change. The experimental data certainly indicate this tendency. Note that due to decoherence caused possibly by the interaction, the oscillations of sublattice populations are damped, which makes it difficult to measure the frequency around the exact BZ edge.

Finally, we experimentally investigate dependence of the band gap on the interaction. The gap energies are measured with various atom numbers. Here, we focus on E_{2-1} along the Γ-X direction (see Fig. 4 (a)). For a uniform, weakly interacting BEC, the chemical potential has linear dependence on the atomic density, leading to $N^{2/5}$ dependence of the central density. Therefore, we plot the observed oscillation frequency as a function of $N^{2/5}$ in Fig. 4 (b), (c), and (d). The data are in good agreement with the calculations for the atom density with half of the maximum value. By extrapolating the experimental data to a small atom number limit, it is also confirmed that the band gap at each quasimomentum approaches the prediction of a single-particle theory.

In conclusion, we have studied an interaction effect on the Bloch bands for superfluids in an optical Lieb lattice. We observed that the 2nd band, which is a flat band in a single-particle description, is significantly

shifted and distorted along the Γ-X direction by the interaction. Further applications of our method include the study of an artificial gauge field, which induces the modification of an energy spectrum and a topologically nontrivial phase for fermions in a Lieb lattice [26]. In addition, our technique demonstrated for an optical Lieb lattice should be used to create and observe an interesting interaction-driven effect such as a swallow tail [27], in which the strong interaction compared with a band gap induces the loop structure in the energy band.

This work was supported by the Grant-in-Aid for Scientific Research of JSPS (No. 25220711, No. 26247064, No. 16H00990, and No. 16H01053), the Impulsing Paradigm Change through Disruptive Technologies (ImPACT) program, JST CREST (No. JPMJCR1673), and H.O. acknowledges support from JSPS.

* Electronic address: hideki_ozawa@scphys.kyoto-u.ac.jp

[1] M. Geisler, J. Smet, V. Umansky, K. von Klitzing, B. Naundorf, R. Ketzmerick, and H. Schweizer, Physica E: Low-dimensional Systems and Nanostructures **25**, 227 (2004).
[2] K. Nakada, M. Fujita, G. Dresselhaus, and M. S. Dresselhaus, Phys. Rev. B **54**, 17954 (1996).
[3] A. P. Schnyder and S. Ryu, Phys. Rev. B **84**, 060504 (2011).
[4] S. D. Huber and E. Altman, Phys. Rev. B **82**, 184502 (2010).
[5] E. H. Lieb, Phys. Rev. Lett. **62**, 1201 (1989).
[6] K. Noda, A. Koga, N. Kawakami, and T. Pruschke, Phys. Rev. A **80**, 063622 (2009).
[7] K. Noda, K. Inaba, and M. Yamashita, Phys. Rev. A **90**, 043624 (2014).
[8] E. Tang, J.-W. Mei, and X.-G. Wen, Phys. Rev. Lett. **106**, 236802 (2011).
[9] K. Sun, Z. Gu, H. Katsura, and S. Das Sarma, Physical Review Letters **106**, 236803 (2011).
[10] T. Neupert, L. Santos, C. Chamon, and C. Mudry, Phys. Rev. Lett. **106**, 236804 (2011).
[11] Y.-Z. You, Z. Chen, X.-Q. Sun, and H. Zhai, Phys. Rev. Lett. **109**, 265302 (2012).
[12] G.-B. Jo, J. Guzman, C. K. Thomas, P. Hosur, A. Vishwanath, and D. M. Stamper-Kurn, Phys. Rev. Lett. **108**, 045305 (2012).
[13] S. Taie, H. Ozawa, T. Ichinose, T. Nishio, S. Nakajima, and Y. Takahashi, Science Advances **1** (2015), 10.1126/sciadv.1500854.
[14] D. Guzmán-Silva, C. Mejía-Cortés, M. A. Bandres, M. C. Rechtsman, S. Weimann, S. Nolte, M. Segev, A. Szameit, and R. A. Vicencio, New Journal of Physics **16**, 63061 (2014).
[15] R. A. Vicencio, C. Cantillano, L. Morales-Inostroza, B. Real, C. Mejía-Cortés, S. Weimann, A. Szameit, and M. I. Molina, Phys. Rev. Lett. **114**, 245503 (2015).
[16] S. Mukherjee, A. Spracklen, D. Choudhury, N. Goldman, P. Öhberg, E. Andersson, and R. R. Thomson, Phys. Rev. Lett. **114**, 245504 (2015).
[17] F. Baboux, L. Ge, T. Jacqmin, M. Biondi, E. Galopin, A. Lemaître, L. Le Gratiet, I. Sagnes, S. Schmidt, H. E. Türeci, A. Amo, and J. Bloch, Phys. Rev. Lett. **116**, 066402 (2016).
[18] I. Bloch, J. Dalibard, and W. Zwerger, Rev. Mod. Phys. **80**, 885 (2008).
[19] P. T. Ernst, S. Götze, J. S. Krauser, K. Pyka, D.-S. Lühmann, D. Pfannkuche, and K. Sengstock, Nature Phys. **6**, 56 (2010).
[20] S. Kling, T. Salger, C. Grossert, and M. Weitz, Phys. Rev. Lett. **105**, 215301 (2010).
[21] M. Ben Dahan, E. Peik, J. Reichel, Y. Castin, and C. Salomon, Phys. Rev. Lett. **76**, 4508 (1996).
[22] N. W. Ashcroft and N. D. Mermin, *Solid State Physics* (W. B. Saunders Co., Philadelphia, 1976).
[23] G. Pettini and M. Modugno, Physical Review A **83**, 013619 (2011).
[24] H. M. Price and N. R. Cooper, Physical Review A **85**, 033620 (2012).
[25] See Supplementary Material, which includes theoretical and experimental details and Refs. [13, 28, 29].
[26] N. Goldman, D. F. Urban, and D. Bercioux, Phys. Rev. A **83**, 063601 (2011).
[27] M. Machholm, C. J. Pethick, and H. Smith, Phys. Rev. A **67**, 053613 (2003).
[28] C. Pethick and H. Smith, *Bose-Einstein condensation in dilute gases* (Cambridge University Press, Cambridge, U.K., 2002).
[29] A. Trombettoni and A. Smerzi, Phys. Rev. Lett. **86**, 2353 (2001).